

Effect of Pulsed Current on Temperature Distribution, Weld Bead Profiles and Characteristics of GTA Welded Stainless Steel Joints

N.Karunakaran

Department of Mechanical Engineering, Annamalai University, Annamalai Nagar – 608002, India.

ABSTRACT

This paper compares temperature distribution and weld bead profiles of constant current and pulsed current gas tungsten arc welded AISI 304L grade stainless steel joints. The effects of pulsed current welding on tensile properties, hardness profiles, micro structural features and residual stress distribution of stainless steel joints are reported. The use of pulsed current technique improves the tensile properties of the welds compared to those of continuous current welds due to grain refinement occurring in the fusion zone.

Keywords: *Stainless steel, gas tungsten arc welding, pulsed current, temperature distribution, bead profiles, tensile properties.*

1. INTRODUCTION

Austenitic stainless steels (ASS) gathered wide acceptance in the fabrication of pipelines, power plants, refineries, pressure vessels, nuclear reactors, building & bridges, automotive, trucks & trains, ships, offshore structures, aerospace structures and microelectronics [1]. In any structural application of this alloy, its weldability is of utmost importance as welding is largely used for joining of structural components. The preferred welding process for stainless steel is frequently Gas Tungsten Arc (GTA) welding due to its comparatively easier applicability and better economy. For the thinner section of this alloy, the pulsed current has been found beneficial due to its advantages over the conventional continuous current process [2].

In conventional welding, fusion zones typically exhibit coarse columnar grains because of the prevailing thermal conditions during weld metal solidification. This often results in inferior weld mechanical properties. Several methods for refining weld fusion zones was tried with some success in the past. Some of them are - inoculation with heterogeneous nucleants, microcooler additions, surface nucleation induced by gas impingement and introduction of physical disturbance through techniques such as torch vibration [3]. Two relatively new techniques namely, magnetic arc oscillation and current pulsing, have gained wide popularity because of their striking promise and the relative ease with which these techniques can be applied to actual industrial situations with only minor modifications of the existing welding equipment [4].

Pulsed current GTA welding, developed in 1950s, is a variation of GTA welding which involves cycling of the welding current from a high level to a low level at a selected regular frequency. The heat energy required to

melt the base material is supplied during peak current pulses for brief intervals of time, this allows the heat to dissipate into the base material leading to a narrower Heat Affected Zone (HAZ). The technique has secured a niche for itself in specific applications such as welding of root passes of tubes, and welding thin sheets, where precise control over penetration and heat input are required to avoid burn through [5].

Extensive research was performed in this process and the advantages reported include improved bead contour, greater tolerance to heat sink variations, lower heat input requirements, reduced residual stresses and distortion [6]. The metallurgical advantages reported in literature include refinement of fusion zone, grain size and substructure, reduced width of HAZ, control of segregation, etc [7]. All these factors will help in improving mechanical properties. Several investigators have used current pulsing to obtain grain refinement in weld fusion zones and improvement in weld mechanical properties [8, 9]. However, reported research work on the effect of pulsed current on temperature distribution, bead profiles and their subsequent influence on tensile properties, hardness profiles and microstructure characteristics are very scant. Hence, the present investigation was carried out to understand the effect of pulsed current welding technique on peak temperature, cooling rate, cross sectional weld bead profile, micro hardness, residual stress distribution, microstructure and the tensile properties of pulsed gas tungsten arc welded AISI 304L stainless steel joints.

2. EXPERIMENTAL PROCEDURE

In this investigation, rolled plates of 4 mm thick AISI grade 304 stainless steel were used as base material. The chemical composition and mechanical properties of base

metal are presented in Table 1. The plates of stainless steel were cut to the required size (150 x 150 mm) by power hacksaw cutting and grinding. Square butt joint configuration was used to fabricate the welded joints. Single pass, autogenous welding procedure (without filler metal addition) was applied to fabricate the joints. High

purity (99.99%) argon gas was used as shielding gas with a flow rate of 9 lpm [8]. 2% Thoriated Tungsten electrode of 3.2 mm diameter was used with DC straight polarity (electrode -ve and weld plate +ve) to carryout the experiments. The arc length was maintained at 2mm [7].

Table 1(a) Chemical composition (wt%) of base metal

C	Mn	Si	P	S	Cr	Ni	N	Fe
0.03	2	0.75	0.045	0.03	18-20	8-12	0.10	Remainder

Table 1(b) Mechanical properties of base metal

Yield Strength (MPa)	Tensile Strength (MPa)	Elongation in 50 mm gauge length (%)	Micro Hardness at 0.05 Kg load (Hv)
205	515	40	280

The experimental setup is shown in figure 1. The Lincoln Electric TIG welding machine controlled the welding parameters, (Model: "Precision TIG 375"). To measure the temperature during welding the K Type Chromel – Alumel thermocouple was used [10] [11] [12]. The hot end diameter of the thermocouple was 1.5 mm, the cold end was fixed to a thermocouple bank and this was in turn connected to the data acquisition system Lab view. Labview was a bundled package on virtual instrumentation having the flexibility to measure the parameter of concern at very short time interval. Figure 2 shows the three positions on the plate to which the thermocouples were glued to a depth was 2mm from the

bottom of the plate [13]. Before welding was performed, the plates were cleaned and thermocouples were incorporated at its appropriate positions. Welding was done by both the constant current (CC) and the pulsed current (PC) process. A number of trial runs on the base material were performed to fix the upper and lower heat input levels.

It is seen from *Lu, and Kou*, [10] that for the TIG welding process, the molten surface is turbulent if the welding current is more than 225 A hence limited to this value. The frequency was fixed at 6 hz [14].

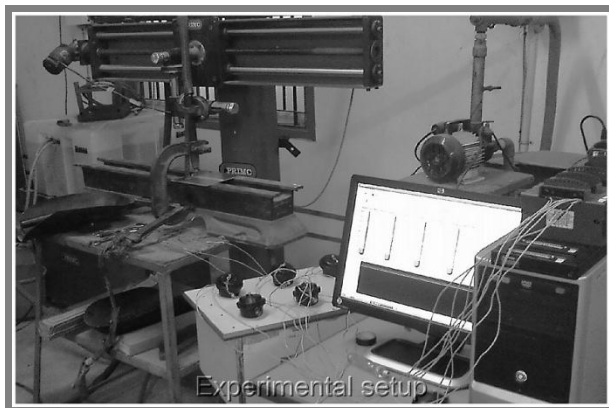


Figure 1. Experimental Setup

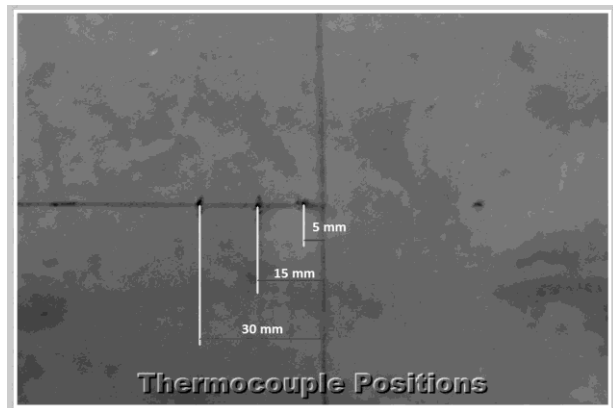


Figure 2. Thermocouple positions

The welding parameters used in the investigation are shown in Table 2. For the calculation of the heat Input (Q) the relationship used for Constant Current process was $Q = \{(V \times I) / n\} \eta$ where V is the voltage, I is the current, n is the welding speed and η is the efficiency of utilization of the heat generated [15] [16]. The computation of heat input in the Pulsed Current process was done by finding the Mean Current using the relationship $I_m = \{(I_p \times t_p) + (I_b \times t_b)\} / t_T$ (where I_m - mean current I_p - peak current I_b - base current t_p - time on peak pulse t_b - time on base current t_T - total time) [16] [17] [18]. The RMS value of current or the effective current was computed and the heat input values tabulated in 2(b). Both the processes were performed at the same speed and the efficiency of utilization of the heat generated was taken as 70% [15] [16]

$t_p) + (I_b \times t_b)\} / t_T$ (where I_m - mean current I_p - peak current I_b - base current t_p - time on peak pulse t_b - time on base current t_T - total time) [16] [17] [18]. The RMS value of current or the effective current was computed and the heat input values tabulated in 2(b). Both the processes were performed at the same speed and the efficiency of utilization of the heat generated was taken as 70% [15] [16]

Table 2(a) Constant Current Welding Parameters

Experiment No	Current (amps)	Voltage (volts)	Welding speed (mm/sec)	Efficiency (%)	Heat Input (Joules/mm)
1	100	12.2	1.974	70	433
2	120	13.5	1.974	70	574
3	140	14	1.974	70	695
4	160	14.1	1.974	70	800
5	180	15.7	1.974	70	1002

Table 2(b) Pulsed Current Welding Parameters

Experiment No	Peak Current (amps)	Base Current (amps)	Voltage (volts)	Pulse on time (%)	Frequency (hz)	Welding speed (mm/sec)	Efficiency (%)	Heat Input (Joules/mm)
1	100	50	12.2	50	6	1.974	70	350
2	120	60	14	50	6	1.974	70	471
3	140	70	13	50	6	1.974	70	510
4	160	80	12.4	50	6	1.974	70	556
5	180	90	13.2	50	6	1.974	70	666

3. RESULTS

3.1 Temperature Profiles

The temperatures at 5mm, 15 mm and 30 mm from the weld bead centre were measured for 600 seconds. The data acquisition system Lab view was used to obtain the

temperatures at an interval of one second [12]. The heating and cooling curves for the various heat input levels are shown in figure 3. The values of peak temperature are presented in table 3. The cooling rate was determined for the temperature drop of 800^o C to 500^o C [19]. The values of the same for the location of 5mm from weld centre are shown in table 3.

Table 3 Peak temperature values

Experiment No	Current (amps)	Heat Input (Joule/mm)		Peak temp at 5 mm (°K)		Cooling Rate (° C/Second)		Peak temp at 15 mm (°K)	
		CC	PC	CC	PC	CC	PC	CC	PC
1	100	433	350	955	661	12.6	*	626	489
2	120	574	471	1052	704	12.6	*	694	518
3	140	695	510	1217	1007	12.3	16.4	711	579
4	160	800	556	1329	1025	10.3	13.7	751	622
5	180	1002	666	1630	1081	9.9	12.6	957	642

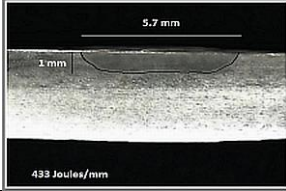
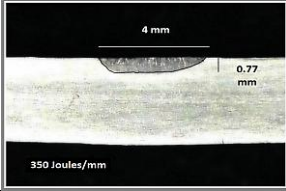
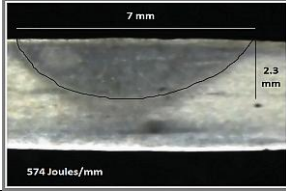
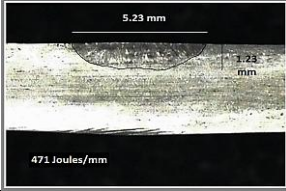
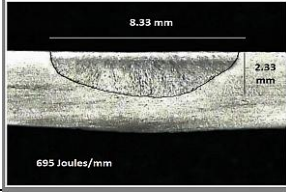
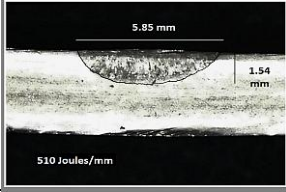
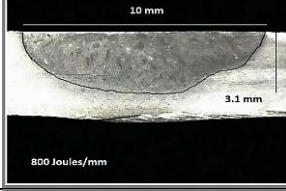
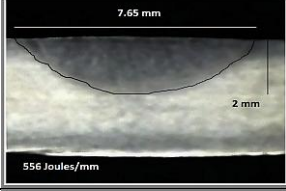
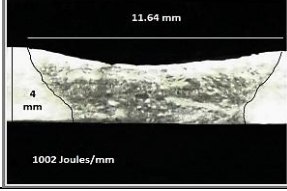
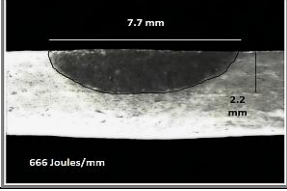
*Peak Temperature below 500^o C

3.2 Bead Profiles

The rate of heat input during welding and the cooling rate after welding strongly influence the grain size and phase formation. Hence it is imperative to understand the effect of various levels of heat input and its influence on the bead profile. Specimens were extracted from the mid

portion of the welded plates. The cross sectional surface were polished using standard metallographic procedures and etched with aqua-reagent to get the clear bead profile. The bead profiles were taken using stereozoom microscope. The weld bead profiles and related dimensions are presented in table 4

Table 4 Cross sectional profile of the weld beads

Current (Amps)	Constant Current (CC)	Pulsed Current (PC)	*P/T		W/P*	
			CC	PC	CC	PC
100			0.25	0.19	5.7	5.2
120			0.58	0.31	3.1	4.3
140			0.58	0.39	3.6	3.8
160			0.77	0.50	3.2	3.8
180			1.00	0.55	2.9	3.5

*P: depth of penetration; W: width of the weld bead; T: plate thickness

4. CHARACTERISTICS OF WELDED JOINTS

The various penetration that was achieved during weld was compared. From the comparison the joint fabricated at 695 J/mm (140 amps) in constant current had a penetration of 2.33 mm that was in par lance with the joint welded at 666 J/mm (180 amps) of pulsed current whose penetration was 2.2 mm. The ratio of penetration to plate thickness was 0.58 and 0.55 for constant current and pulsed current respectively. The ratio of width to penetration was 3.5 and 3.6 for constant current and pulsed current respectively. Hence these two joints exhibited similar physical characteristics. The various

other characteristics of the weld like the tensile properties, microhardness, microstructure and the residual stress are compared for these two joints.

4.1 Tensile Properties

The transverse tensile properties of the welded joints were measured using the Universal Testing Machine (UTM). The 4mm thick welded plates were machined (ground) to 2.5mm thin sheets in order to have full penetration joints. The specimens were prepared as per the ASTM E8-04 standards and three specimen for each joint were tested and the values are presented in Table 5.

Table 5 Tensile properties of the welded joints

Process / Heat Input	Yield strength (MPa)	Tensile strength (MPa)	Elongation (%)	Failure Location
CC / 695 J/mm	375	456	30	Weld centre
PC / 666 J/mm	418	501	33	Weld centre

4.2 Hardness

A microhardness testing machine (SHIMADZU HMV-2 Version 2.02) was used to measure the hardness at the weld bead, 5mm and 15 mm from the weld centre. A load

of 50g was applied for 15 seconds, to obtain the Vickers hardness HV/0.05. Table 6 shows the Vickers hardness values for the two joints at weld zone, 5mm and 15mm from weld bead centre for constant current and pulsed current.

Table 6 Microhardness (Hv) of weldments

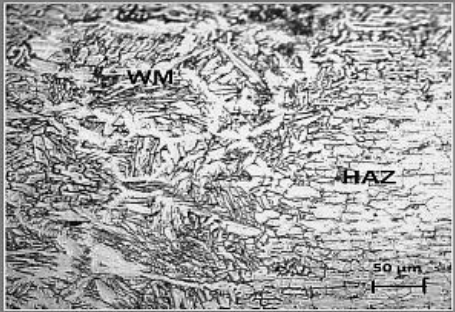

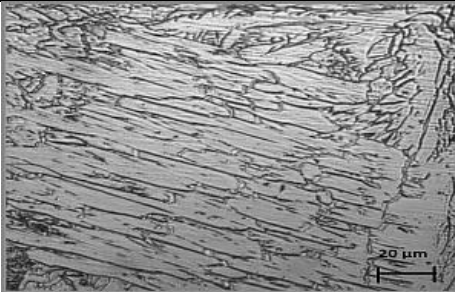
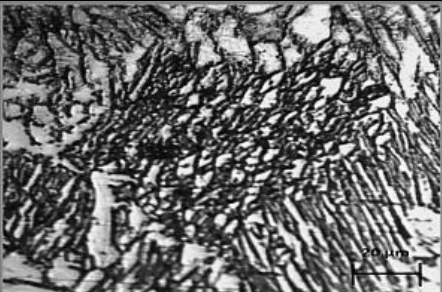
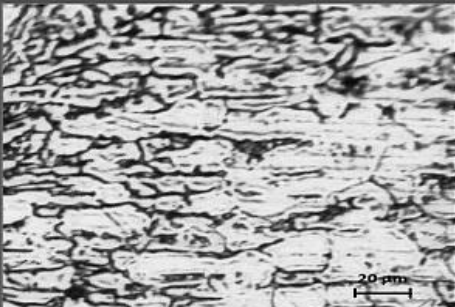
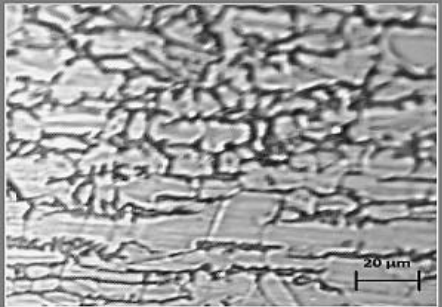
Process / Heat Input	Weld centre	5mm from weld centre	15 mm from weld centre	Base Metal
CC / 695 J/mm	228	240	264	280
PC / 666 J/mm	250	260	270	280

4.3 Microstructure

The strength of the weld metal is characterized by the grain size and the phases present in the microstructure, the phase formation and grain growth are highly influenced by the thermal cycle of the welding operation, the region of interest would be the weld metal and the interface zones because at the weld metal the temperature goes to the peak and cools rapidly thus formation of finer grain sizes

are attributed to this zone. The welded specimen was prepared using the standard metallographic procedure, the polished surfaces were etched with aqua-reagent to get the clear microscopic view of the weldment. The Microscope MEIJI Japan Model MIL7100 was used with the software Metalvision MVLx 1.0. The results of the microstructure at the Interface region, the weld centre and the Heat Affected Zone (HAZ) are presented in table 7.

Table 7 Microstructure of the welded joints

Region	CC / 695 J/mm	PC / 666 J/mm
Inter- face (WM- HAZ)		
Weld centre		
HAZ		

4.4 Residual Stress

The residual stress distribution in the transverse direction was measured by the X ray diffraction method. The equipment used to measure the stress was X3000 Ver 1.22.9 the software Stress tech was used to compile the value of stress from the measured value of “d” in the

Bragg’s equation. The residual stress was measured for one specimen in each of the two process and at the weld bead, 5mm and 10mm from the weld bead centre. The values of the residual stress are presented in table 8. The 0 degrees is the longitudinal stress and the 90 degree is the transverse stress at the points specified.

Table 8 Residual Stress (MPa) distribution

Process / Heat Input	Weld centre		5mm from weld centre		15 mm from weld centre		Base Metal	
	0°	90°	0°	90°	0°	90°	0°	90°
CC / 695 J/mm	+158.7	170	+90	110	+30	50	-80	-65
PC / 666 J/mm	+125	140	+70	90	+10	30	-76.5	-60

5. DISCUSSION

5.1 Effect of Pulse Current on Temperature Profile

The total time of welding was 76 seconds. It is seen that when the torch was nearing the line of thermocouple the maximum temperatures were obtained in all the cases.

The peak temperature increases as the heat input increases in all the cases. In constant current the highest temperature was 1630 K for the higher heat input of 1002 J/mm and the lowest was 955 K for 433 J/mm at the 5mm distance (Fig 3a). In the Pulsed current for the 5mm distance the highest temperature was 1081 K for the heat input of 666 J/mm and lowest peak temperature of 661 K for a heat input of 350J/mm (Fig 3c).

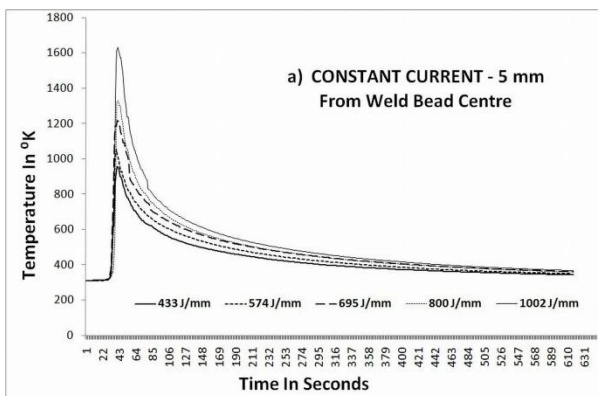


Figure 3 (a). Heating and cooling curve – CC 5mm

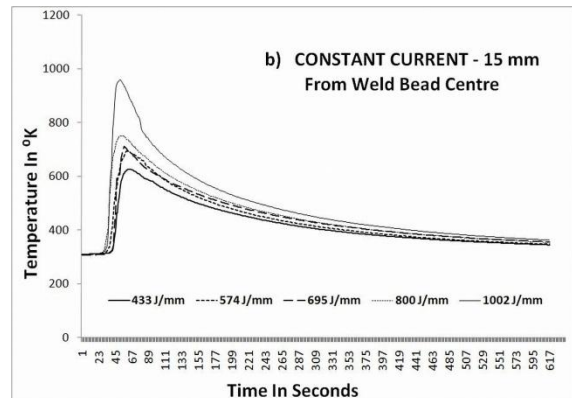


Figure 3 (b). Heating and cooling curve – CC 15mm

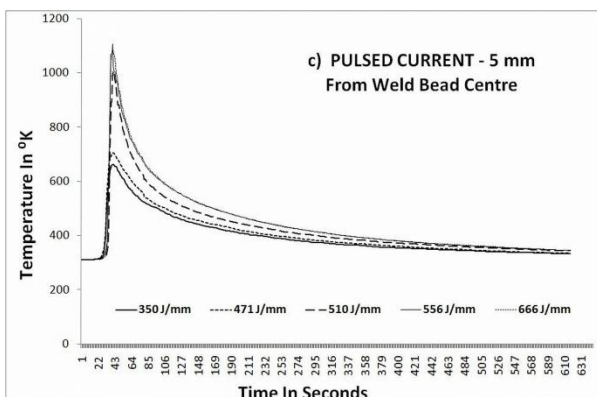


Figure 3 (c). Heating and cooling curve – PC 5mm

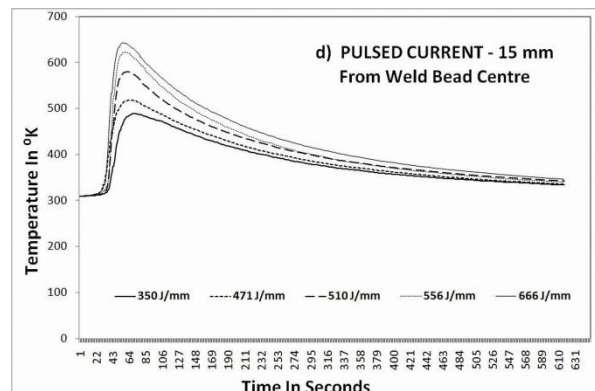


Figure 3 (d). Heating and cooling curve – PC 15mm

From the temperature profiles, closer to the weld bead (5mm) it was seen that for pulsed current conditions the heat input of 500J/mm and above the peak temperatures tend to cluster together and was in the range of about 1000K. The heat input of lesser than 500J/mm saw a lower peak temperature of less than 650 K. The reason for this can be attributed to the temperature dependent properties of SS304. This was not seen in the constant current process, the peak temperature varied with heat input variation.

The profiles of temperature at 15 mm from the weld centre for constant current and pulsed current followed a similar pattern. The pulsed current showed more uniform cooling pattern, while the constant current saw a clustering at 560 to 700 K for heat inputs of 400 – 800 J/mm, which were similar to the profiles of 5mm. The reasons for this clustering can be attributed to the various thermal properties of AISI 304, The Linear Expansion (dL/L) unit less value turns positive at 560 K, and the specific heat of the material rises steeply after 600 K.

The cooling rate presented in table 3 shows that for the lower heat input rates the cooling rate is faster and for higher heat inputs the cooling rate is slower, for the lowest heat input the cooling rate for constant current is 12.6 °C/Second and for highest heat input it is 9.9 °C/Second. For the pulsed current the lower heat inputs did not generate temperatures higher than 500°C but for the 140 amps of current the cooling rate was 16.4 °C/Second and for the highest heat input level the cooling rate was 12.6 °C/Second. It is seen that the cooling rate for pulsed current is much higher than that of the constant current.

5.2 Effect of Pulsed Current on Bead Profile

It is seen from table 4 that for the constant current for the lower heat input the penetration was about one fourth of the thickness of the plate but when the heat input was raised above 800 J/mm the instance of burn through occurred. The profile of the pulsed current were more controlled and the penetration was about one half of the plate thickness. The penetration to width ratio for the constant current was higher than that of the pulsed current except at the lower heat input wherein the value was 0.19. For all other heat input the value was around 0.35 and 0.25 for constant current and pulsed current respectively. The effect of the surface tension and buoyancy forces are seen clearly in the lower heat input profile of constant current but seen in all the cases of the pulsed current.

5.3 Effect of Pulsed Current on Tensile properties and Hardness

The tensile properties were compared for the equal penetration welds. In both the cases the cooling rate was

12.3 and 12.6 °C/second at 5 mm from weld bead centre, the heat input was 666 J/mm and 695 J/mm. The yield strength for the constant current was 375 MPa but for pulsed current it was higher at 418 MPa and tensile strength followed the same trend as 456 and 501 MPa for the constant current and pulsed current respectively. The higher strength is seen in the joint fabricated by the pulsed current.

The micro hardness of the base metal was at 280 Hv. It was evident that in both the cases the hardness was the least at the weld centre and gradually increased at the 5mm point and further increased at the 15 mm point. The values of the hardness was less in the constant current joints compared to the pulsed current in all the locations. The peak temperature reached for the constant current was 1217° K and for the pulsed current 1081° K at 5mm distance from weld centre. The reason for the decrease in the hardness can be attributed to the variation in the temperatures attained. Due to the pulsing of current in the joint fabricated by the pulsed current the huge drop in the peak temperature is seen. Hence the higher hardness is attributed by the joints fabricated by pulsed current.

5.4 Effect of Pulsed Current on Microstructure

The weld metal reveals a structure with vermicular delta ferrite segregated in the grain boundary of austenite matrix. The microstructure of the weld centre reveals coarse grains in the constant current joint while for the pulsed current the grains are fine, the dendrites spacing in the constant current is wider but the pulsed current reveals narrower spacing. It is also seen that the area of grain boundary is much lesser in the constant current compared to that of the pulsed current. The interface region for the pulsed current joint shows vermicular ferrite along the grain boundaries. The ferrite morphology can be attributed to the preferential primary ferrite solidification. The dendrites in the solid liquid region are small and close in both the cases. The effect of higher cooling rate is seen in the microstructure of the pulsed current specimen with domination of smaller grains. The morphology of the constant current predominates with the columnar grain structure due to the lower cooling rate.

Furthermore, the temperature fluctuations inherent in pulsed welding lead to a continual change in the weld pool size and shape favouring the growth of new grains. It is also to be noted that effective heat input for unit volume of the weld pool would be considerably less in pulse current welds for which reason the average weld pool temperatures are expected to be low [19].

It is important to note that while dendrite fragmentation has frequently been cited as a possible mechanism,

evidence for the same has not been hitherto established / demonstrated. It has been sometimes suggested that the mechanism of dendrite break-up may not be effective in welding because of the small size of the fusion welds and the fine interdendrite spacing in the weld microstructure. Thus grain refinement observed in the pulsed current welds is therefore believed to be due to other effects of pulsing on the weld pool shape, fluid flow and temperatures [20].

5.5 Effect of Pulsed Current on Residual Stress

It is seen from the results that both the specimen showed tensile stress at the weld centre, 5 mm and 15 mm. The base metal had compressive stress. The weld centre had higher values of tensile stress and decreased further away from it. The value of stress at the weld centre for the constant current was 158 MPa while that of Pulsed current was 125 MPa. This trend was seen in points at 5mm and 15 mm from weld centre. The joints fabricated by the Pulsed current showed lesser residual stress compared to that of constant current. The reason for this characteristic feature can be attributed to the lesser peak temperature attained during welding of the constant current joints and the higher cooling rate $12.6^{\circ}\text{C}/\text{second}$ that was achieved in the pulsed current welds.

6. CONCLUSION

From this investigation, it was found that

- (i) The pulsed current welding technique recorded lower peak temperatures for the specimens compared (constant current at heat input of 695J/mm the peak temperature was 1217K; pulsed current at heat input of 666J/mm the peak temperature was 1081K). Lower magnitude of residual stresses were seen in pulsed current compared to constant current welding, which is highly preferable for thin sheet welding.
- (ii) The gas tungsten arc welded stainless steel joint fabricated by pulsed current welding technique exhibited superior tensile properties compared to constant current welding technique.
- (iii) The formation finer grains and fragmentation of dendrites caused by pulsed current are the main reasons for enhanced tensile and hardness properties of the joints.

ACKNOWLEDGEMENT

The author wish to express his sincere thanks to the, Department of Manufacturing Engineering, Annamalai University, Annamalai Nagar 608002 for the facilities

provided to carry out this investigation. The author also wishes to acknowledge Dr V. Balasubramanian, Director CMAJOR and Professor for extending support and guidance throughout the work.

REFERENCES

- [1] **G. Lothongkum, E. Viyanit, P. Bhandhubanyong** Study on the effects of pulsed TIG welding parameters on delta-ferrite content, shape factor and bead quality in orbital welding of AISI 316L stainless steel plate. *Journal of Materials Processing Technology* 2001 Vol 110 233 – 238.
- [2] **Prasad Rao K, G.M. Reddy and A.A. Gokhale** Grain refinement and improvement of strength and ductility of welds by pulsed current and magnetic arc oscillation techniques, *International Welding Conference*, New Delhi, 1999 : 1050-1055.
- [3] **Davies CJ and JG Garland.** Solidification structures and properties of fusion welds. *Int. Mater. Review*, 1975, **Vol 20**, 83-106.
- [4] **Kou S and Y.Le** Nucleation mechanism and grain refining of weld metal, *Welding Journal*, 1986, **Vol 65**, 305s – 313s.
- [5] **Madhusudhan Reddy G, Gokhale A.A and Prasad Rao K** Optimization of pulse frequency in pulsedcurrent gas tungsten arc welding of aluminium – lithium alloy sheets, *Journal of Material Science &Technology*, 1998, **Vol. 14**, 61-66
- [6] **Shinoda T, Ueno Y and Masumoto I** Effect of pulsed welding current on solidification cracking in austenitic stainless steel welds, *Transac. of the Japan Welding Soc.*, 1990, **Vol. 21**, :18-23.
- [7] **Mohandas T and Madhusudhana Reddy G** Effect of frequency of pulsing in gas tungsten arc welding on the microstructure and mechanical properties of titanium alloy welds, *Jl. of Mater SciLetters*, 1996, **Vol. 15**, 626-628.
- [8] **V.Balasubramanian, V.Ravisankar and G.Madhusudhan Reddy**, Effect of pulsed current and postweld aging treatment on tensile properties of argon arc welded high strength aluminium alloy, *Materials Science and Engineering – A*, 2007, **Vol.459**, 7-18.
- [9] **M.Balasubramanian, V.Jayabalan and V.Balasubramanian**, A mathematical model to predict impact toughness of pulsed current gas tungsten arc welded titanium alloy, *International*

Journal of Advanced Manufacturing Technology, 2008, **Vol.35**, 852-858.

- [10] **Lu, M., Kou, S.**, Power and current distribution in Gas Tungsten Arcs. *Weld. J.* 1988, **Vol 67(2)** 29s–33s.
- [11] **Sadek C, Absi Alfaro, K S Chawla & John Norrish** “Computer Based Data Acquisition for welding research and production” *Journal of Materials Processing Technology*, 1995, **Vol 53**, 1-13
- [12] **Peter R.N. Childs** “Practical Temperature Measurements” *Elsevier Publications*. 1998
- [13] **M. Sunar , B.S. Yilbas , K. Boran** “Thermal and stress analysis of a sheet metal in welding” *Journal of Materials Processing Technology*, 2006, **Vol 172**, 123–129.
- [14] **Paul Scott**, “Selecting a welding frequency” article at <http://www.thermatool.com/>.
- [15] **C.V. Gonsalves, L.O. Vilarinho, A. Scotti, G. Guimaraes** “Estimation of heat source and thermal efficiency in GTAW process by using inverse techniques” *Journal of Materials Processing Technology*. 2006, **Vol 172**, 42–51
- [16] **W.-H. Kim, S.-J . Na** “Heat and fluid flow in pulsed current GTA weld pool” *International Journal of Heat and Mass Transfer* 1998, **Vol 41**, 3213-3227
- [17] **H.G. Fan, Y.W. Shi , S.J. Na** “Numerical analysis of the arc in pulsed current gas tungsten arc welding using a boundary-fitted coordinate” *Journal of Materials Processing Technology* 1997, **Vol 72**, 437–445.
- [18] **G. Lothongkum, P. Chaumbai, P. Bhandhubanyong** “TIG pulse welding of 304L austenitic stainless steel in flat, vertical and overhead positions” *Journal of Materials Processing Technology* 1999, **Vol 89** - 90 410 – 414.
- [19] **V.Ravisankar and V.Balasubramanian**, Optimising the pulsed TIG welding parameters to refine the fusion zone, *Science and Technology of Welding & Joining*, 2006, **Vol.11, No.6**, 112-116
- [20] **Norman A.F, Hyde K, Costello F, Thompson S, Birley S and Pragnell P.B** Examination of the effect of Sc on 2000 and 7000 series aluminium castings: for improvements in fusion welding, *Materials Science and engineering*, 2003, **Vol A 354**, 188-198.